

1
2
3
4
5
6
7
8
9
10
11
12
13
14
15
16
17
18
19
20
21
22
23
24
25
26
27
28
29
30
31
32
33
34
35

NAADP binding proteins find their identity

Jonathan S. Marchant^{1*}, Gihan S. Gunaratne¹, Xinjiang Cai²,
James T. Slama³ and Sandip Patel^{4*}

¹Department of Cell Biology, Neurobiology & Anatomy, Medical College of Wisconsin, 8701 Watertown Plank Road, Milwaukee, WI 53226

²Division of Cardiology, Department of Medicine, David Geffen School of Medicine at UCLA, Los Angeles, CA, USA

³Department of Medicinal & Biological Chemistry, University of Toledo College of Pharmacy and Pharmaceutical Sciences, 3000 Arlington Avenue, Toledo, OH 43614

⁴Department of Cell and Developmental Biology, University College London, Gower Street, London WC1E 6BT, UK

* Co-corresponding Authors:

JMarchant@mcw.edu

patel.s@ucl.ac.uk

6 elements allowed: Figures=4 (Key Figure=Figure 1). Boxes=2.

Keywords: calcium signaling; endosomes; lysosomes; cancer; photoaffinity probes

ORCID IDs

JSM 0000-0001-6592-0877

GSG 0000-0002-1094-5820

XC 0000-0001-8933-7133

JTS 0000-0001-6053-1522

SP 0000-0001-7247-2013

SOCIAL MEDIA @MarchantLab

36 **Abstract**

37 Nicotinic acid adenine dinucleotide phosphate (NAADP) is a second messenger that
38 releases Ca^{2+} from endosomes and lysosomes by activating ion channels called two
39 pore channels (TPCs). However, no NAADP binding site has been identified on TPCs.
40 Rather, NAADP activates TPCs indirectly by engaging NAADP-binding proteins
41 (NAADP-BPs) that form part of the TPC complex. After a decade of searching, two
42 different NAADP-BPs were recently identified: Jupiter microtubule-associated homolog
43 2 (JPT2) and Like-Sm protein 12 (LSM12). These discoveries bridge the gap between
44 NAADP generation and NAADP activation of TPCs, providing new opportunity to
45 understand and manipulate the NAADP signaling pathway. The unmasking of these
46 NAADP-BPs will catalyze future studies to define the molecular choreography of the
47 NAADP-signaling pathway.

48 **NAADP-mediated Ca²⁺ signaling via two-pore channels: Bridging the gap**

49

50 **Nicotinic acid adenine dinucleotide phosphate (NAADP;** see Glossary) is a second
51 messenger that releases Ca²⁺ from acidic organelles in numerous cell types, and it acts
52 in the nanomolar range to regulate many diverse cellular processes [1]. NAADP exerts
53 these effects by activating **two-pore channels (TPCs)**, an ancient family of eukaryotic
54 intracellular ligand and/or voltage-gated ion channels localized within the
55 endolysosomal system [2]. TPCs are Ca²⁺- and Na⁺-permeable channels, with TPC1
56 and TPC2 expressed in human cells [3, 4]. TPCs control subcellular trafficking events
57 through the endolysosomal system [5], regulating the uptake of physiological
58 substrates, as well as pathogen internalization. They also play a key role in
59 environmental sensing [6]. TPC activity is controlled through the coordinated action of
60 several regulatory inputs (**Figure 1A**). Activators include both NAADP, which releases
61 endolysosomal Ca²⁺, and phosphatidylinositol 3,5-bisphosphate (PI(3,5)P₂), which
62 evokes a highly-selective Na⁺ current, as well as membrane voltage [3, 7-9]. The
63 behavior of the channel likely switches between these modalities with specific functional
64 outcomes being keyed to the nature of the activating stimulus [10].

65

66 One of several challenges related to our understanding of these versatile ion channels,
67 and the progression of TPCs as druggable entities, has been a fundamental gap in our
68 knowledge of how TPCs are activated by NAADP. We know TPCs are directly gated by
69 PI(3,5)P₂ through an atomically resolved binding site [11-13]. But, in stark contrast, no
70 NAADP-binding site has been resolved on the TPC itself. Rather, it was thought NAADP
71 activates TPCs indirectly by binding to an unidentified **NAADP-binding protein**
72 (**NAADP-BP**) associated with the TPC complex (**Figure 1B**).

73

74 The molecular identity of this NAADP-BP has remained unknown for a decade.
75 However, recent breakthroughs now provide the field with a surfeit of riches, as two
76 unique NAADP-BP candidates have been identified within the last year. These two
77 proteins, **Jupiter Microtubule Associated Homolog-2 (JPT2)** and **'like-Sm' protein**
78 **12 (LSM12)**, both bind NAADP, interact with TPCs, and are necessary to support

79 endogenous NAADP-evoked Ca^{2+} signals [14-16]. They provide considerable new
80 impetus for understanding NAADP action. Therefore, it is timely to review how
81 identification of these NAADP-BPs defines new questions and trajectories for research
82 that will further our mechanistic understanding of NAADP signaling. In this review, we
83 focus predominantly on JPT2, given our role in identifying this NAADP-BP [14]. After
84 introducing how JPT2 was discovered, five areas will be explored (**Figure 1C**) relating
85 to (1) the mechanisms by which JPT2 interacts with NAADP and TPCs; (2) the
86 landscape of JPT2 expression and how this is regulated to determine cellular NAADP
87 sensitivity, (3) how a broader understanding of JPT2 interactors and their cellular
88 physiology will expand our knowledge of the cellular functions of NAADP, (4) the
89 broader family of NAADP-BPs, including the recent identification of LSM12 [16] and
90 finally (5) how this knowledge will catalyze development of new tools and drugs to
91 manipulate this signaling pathway. While JPT2 is the core focus of this review, many of
92 the themes are also applicable to the study of LSM12 [16], which is highlighted
93 separately in its own section.

94

95 **Identification of JPT2 as an NAADP-BP**

96 Sea urchin eggs have been an indispensable model system for studying NAADP action
97 because it is a simple experimental preparation that exhibits robust, highly reproducible
98 Ca^{2+} responses to NAADP as well as other Ca^{2+} -mobilizing second messengers [17,
99 18]. Soon after the Ca^{2+} -mobilizing properties of NAADP were first discovered in this
100 invertebrate preparation, radiolabeled NAADP (^{32}P -NAADP, **Box 1**) was used to identify
101 stereoselective binding sites for NAADP [19, 20]. This approach was subsequently
102 extended to mammalian tissues [21, 22]. However, it took another decade to identify
103 TPCs as NAADP targets [3, 4, 23]. The subsequent realization that TPCs do not bind
104 NAADP grew from this work but was directly evidenced from photolabeling studies
105 using NAADP-based photoprobes. Specifically, use of a photoreactive analog of ^{32}P -
106 NAADP (^{32}P -5-azido-NAADP, **Box 1**) to resolve NAADP-binding targets revealed
107 specific photolabeling of a ~23kDa protein band considerably smaller than the TPCs
108 [24-26]. The photolabeling characteristics of this low molecular weight NAADP-BP
109 revealed: (i) a diagnostic pharmacology of NAADP-evoked Ca^{2+} release, (ii) the

110 expected selectivity for NAADP versus NADP, and (iii) irreversible binding in high K^+ , all
111 features of NAADP messenger action established from earlier work [24, 25]. Observed
112 affinities of NAADP binding sites, measured by photoaffinity labeling (PAL) or ^{32}P -
113 NAADP binding, were also identical [24, 25]. These findings were subsequently shown
114 to be consistent across various mammalian cell lines, primary cells, and tissues [9, 27].
115 Further, the ~23kDa NAADP-BP was definitively shown to be distinct from TPCs as
116 photolabeling persisted in TPC knockout mice even though NAADP binding was
117 preserved [9, 25].

118

119 Despite considerable efforts with the initial photoprobe, as well as synthesis and testing
120 of iterated versions [28, 29], it proved challenging to enrich this elusive NAADP-BP
121 sufficiently to narrow down the long list of candidates collated from mass spectrometry
122 datasets [30, 31]. It was the development of a second-generation **bifunctional**
123 **photoprobe** (^{32}P -alkyne-‘all-in-one-click’(AIOC)-NAADP, **Box 1**), which retained the
124 photoactivatable azide group but incorporated an additional ‘clickable’ alkynyl moiety to
125 couple photoaffinity labeling with an enrichment strategy, that broke the status quo. This
126 probe, when utilized in erythrocytes – a cell type with strong, selective photolabelling of
127 the ~23kDa NAADP-BP – resulted in our identification of JPT2 [14]. Further support that
128 JPT2 acts as an NAADP-BP includes: (i) knockdown of endogenous JPT2 reducing the
129 intensity of the photolabeled NAADP-BP in mammalian cell lines, and strongly inhibiting
130 endogenous NAADP-evoked Ca^{2+} signals mediated by TPCs and (ii) co-
131 immunoprecipitation studies demonstrating that JPT2 interaction was biased toward
132 TPC1 compared with TPC2 [14]. JPT2 was also isolated from another blood cell (Jurkat
133 T cells) by Roggenkamp *et al.* using a sequential purification protocol to track
134 radioactivity associated with the photolabeled NAADP-BP targets [15, 32].

135

136 Human JPT2 exists as three splice isoforms that differ in their N-termini (**Figure 2A**)
137 [33]. Their predicted molecular weights match well the 22-23 kDa species labelled in
138 photolabeling experiments. Additionally, JPT1 is a related protein displaying ~30%
139 sequence identity [33]. **Figure 2B** displays an updated phylogeny of JPT homologues in
140 animals [33]. JPT2 appears to be a vertebrate invention present in basal vertebrates

141 such as *Petromyzon marinus* (sea lamprey). JPT1 is also present in major vertebrate
142 classes as well as in *Anneissia japonica*, an echinoderm (sub-phylum, Crinozoa).
143 However, JPT homologues in other echinoderms such as sea urchins and a number of
144 additional chordate subphyla and protostomes, group as an independent clade.
145 Whether these homologues represent ancestral forms of JPT1 or JPT2 remains to be
146 established. This is particularly pertinent in echinoderms where the Ca²⁺-mobilizing
147 effects of NAADP were originally documented.

148

149 **JPT2 and its interaction with NAADP and TPCs**

150 Two key questions emerge from the identification of JPT2 as an NAADP-BP and TPC
151 accessory protein. First, how does NAADP bind to JPT2? Second, how does JPT2 bind
152 TPCs?

153

154 Towards the first question, the JPT2 sequence does not possess any consensus
155 nucleotide binding domains. Instead, it has a repeat structure (much like TPCs) and it is
156 predicted to be a disordered protein. It is also predicted to be modified by a variety of
157 post-translational modifications in mammalian systems, such as phosphorylation. Some
158 of these sites have been validated experimentally and associated with the activity of
159 specific kinases [34]. Thus, NAADP binding may be subject to phosphoregulation.
160 Further work to analyze the properties of JPT2 *in vitro* is needed to define these
161 properties and their impact on NAADP association.

162

163 Regarding the second question, understanding how JPT2 associates with TPCs is
164 critical to establish as it is key to understanding how NAADP-evoked Ca²⁺ signals
165 initiate. A variety of models can be envisaged. For example, increases in cellular
166 NAADP levels may cause a translocation of NAADP-liganded JPT2 to TPCs to trigger
167 activation (**Figure 1Bi**). Alternatively, (a fraction of) JPT2 may be pre-bound to TPCs
168 with NAADP binding, causing a conformational change that opens TPCs (**Figure 1Bii**).
169 That NAADP can gate TPCs in excised patches [35] and in lipid bilayers (following
170 incorporation of purified TPCs or TPC-expressing vesicular preparations) [36, 37]
171 supports a tight association of JPT2 with TPCs. If so, dissociation of JPT2 upon NAADP

172 binding may inactivate the complex (**Figure 1Biii**). Could such dissociation underpin the
173 biphasic NAADP concentration-dependent relationship whereby micromolar
174 concentrations of NAADP *decrease* channel activation [38]?

175
176 From our work, JPT2 seems to preferentially interact with TPC1 over TPC2 [14]. TPC1
177 expression is biased endosomally and TPC2 is considered more lysosomal in human
178 cells. NAADP-BP specificity for TPC isoforms could therefore serve to regionalize
179 NAADP action to a subset of acidic Ca²⁺ stores, providing a route for JPT2 to selectively
180 modify endosomal function and trafficking. Looking beyond TPCs as NAADP-BP
181 targets, Roggenkamp *et al.* show that JPT2 also interacts with ryanodine receptors
182 (RyR1) in T lymphocytes during the initial stages of T cell activation [15]. These data
183 suggest a broader promiscuity of JPT2 beyond the canonical channel (TPC) and
184 organellar target (acidic Ca²⁺ stores), such that JPT2 may be competent to confer
185 NAADP-sensitivity to multiple families of intracellular Ca²⁺ channels [26, 39]. It should
186 be noted that TPC1 and RyR1 are highly dissimilar proteins; therefore, this highlights an
187 issue of whether these associations are mediated directly or through a common
188 intermediary. Elucidation of the diversity of Ca²⁺ channel targets of JPT2 will be
189 necessary for comprehensively decoding NAADP action on intracellular Ca²⁺ dynamics.

190

191 **JPT2 expression and cellular NAADP sensitivity**

192 Some cell types show strong responses to NAADP, some do not. Some preparations
193 respond robustly to NAADP (intact cells), some (broken cell preparations) do not [26,
194 40-42]. If NAADP-BPs are essential for NAADP action on intracellular Ca²⁺ channels,
195 then the presence and properties of NAADP-BPs within a cell at any given point in time
196 will determine cell sensitivity to NAADP. Consequently, regulation of pathways that
197 control expression, properties, and local concentration of NAADP-BPs in the vicinity of
198 TPCs will control when and where NAADP triggers endogenous Ca²⁺ signals. What do
199 we know about JPT2 expression, and how JPT2 expression levels are controlled?

200

201 RNA-sequencing (RNAseq) and protein expression databases evidence that full length
202 JPT2 is broadly expressed in human tissues and cell lines [14], consistent with prior

203 profiling of JPT2 expression [33, 43]. The gene nomenclature for JPT2 (*JPT2/HN1L*)
204 derives for shared molecular homology with JPT1 (*JPT1/HN1*, hematopoietic- and
205 neurological-expressed sequence 1), named based upon a high level of expression in
206 hematopoietic cells and fetal brain tissue [44]. Like JPT1, JPT2/HN1L messenger RNA
207 (mRNA) is also present in multiple brain regions with highest levels in the spinal cord
208 [45]. These observations are of interest given a documented role for NAADP in
209 maturation of spinal neuronal circuitry [46]. Another study identified JPT2 as a highly
210 expressed gene in neuronal stem cells and progenitors [43], which is again intriguing
211 given the observed role of NAADP in neuronal differentiation [47, 48]. How JPT2 levels
212 change during development and how such changes correlate with the timing and
213 localization of endogenous NAADP-evoked Ca^{2+} signals merits resolution. Towards this
214 understanding, transcriptomic analyses of JPT2 expression (**Figure 3A**) show (with the
215 usual caveats of RNA to protein conversion [49]) that JPT2 is not an abundant cellular
216 protein (median range of 4-129 transcripts per million (TPM) for JPT2, [45]). JPT2
217 expression is, however, higher in cell types (SKBR3 and U2OS cells) commonly used to
218 study NAADP-evoked Ca^{2+} signals [14]. Further, expression profiling suggests the
219 abundance and variation in JPT2 levels better correlates with the expression profile of
220 TPC1 than TPC2 (**Figure 3B**), consistent with observations that JPT2 preferentially
221 interacts with TPC1, as described above [14].

222
223 The unmasking of JPT2 as an NAADP-BP permits the relationship between JPT2
224 expression and cellular NAADP sensitivity to be assessed experimentally. In cell types
225 where JPT2 expression is low, can JPT2 overexpression enhance NAADP
226 responsiveness? Reciprocally, does knockdown/knockout of JPT2 impair NAADP action
227 in different cell types and tissues? It has been challenging to demonstrate NAADP
228 sensitivity in permeabilized cells, or by using organelle-based electrophysiological
229 approaches, due to the potential loss of NAADP-BPs from the experimental assay
230 systems. This roadblock has hampered study of TPC properties. If the explanation for
231 the loss of NAADP sensitivity in broken cell preparations is simply the loss of NAADP-
232 BPs required for NAADP action, then tethering NAADP-BPs to TPCs through molecular

233 linkers designed into recombinant NAADP-BP:TPC expression constructs could test this
234 possibility and facilitate the study of NAADP action on TPCs [50].

235

236 How are JPT2 expression levels controlled? JPT2 expression is likely determined by
237 mechanisms controlling gene transcription, mRNA stability, and degradation. Our
238 knowledge of these processes for JPT2 is currently quite limited. We do know that
239 microRNA (miR)-212-5p, which is implicated in cancer progression [51] and Parkinson's
240 disease [52], binds within the 3' untranslated region (UTR) of JPT2, with JPT2
241 expression being inversely correlated with miR-212-5p levels in hepatic cancer [53].
242 JPT2 is also predicted to be modified by various post-translational modifications and
243 interaction with binding partners may provide another way to regulate NAADP-BP
244 levels. Understanding these processes may afford new opportunity for therapeutic
245 approaches to control NAADP action.

246

247 **Other JPT2 functions**

248 Identification of JPT2 as an NAADP-BP establishes an unexpected new functionality to
249 this protein. The existing literature surrounding JPT2 is currently small but highlights
250 roles in viral infection and cancer. This association is intriguing given growing evidence
251 of a role for TPCs in both these areas [14, 54-59], summarized in **Box 2**. Do the known
252 cellular roles of JPT2 extend our understanding of NAADP action into novel aspects of
253 cellular physiology?

254

255 *Viral infection*

256 The first area of functional convergence concerns viral infection. TPCs regulate viral
257 internalization pathways into cells, as shown by experiments using spike-pseudotyped
258 coronaviruses [14, 58, 60] that report translocation through the endolysosomal system.
259 Indeed, knockdown of JPT2 inhibited cellular infectivity of a SARS-CoV-2 pseudovirus,
260 an effect phenocopied by either genetic (small interfering RNA (siRNA)) or
261 pharmacological inhibition of TPCs [14]. Interestingly, this outcome was not mimicked
262 by siRNA of JPT1, which may imply that JPT1 is unlikely to be an NAADP receptor [14].
263 A role for JPT2 in curtailing apoptosis in response to viral infection has also been

264 demonstrated [43]. Further, JPT2 may regulate viral egress from cells as it has been
265 shown to localize to virus-like particles during their exit from host cells [61]. . The role of
266 JPT2 in host responses to viral infection and immune surveillance will be an area of
267 increasing focus [6, 62].

268

269 *Cancer*

270 The second area of functional convergence between JPT2 and TPC function is in
271 cancer. JPT2/HN1L has been implicated in cancer progression in breast cancer [63-65],
272 non-small cell lung cancer [66, 67], hepatocellular carcinoma [53], and adenocarcinoma
273 [68], and bioinformatic analyses confirm JPT2 mRNA is upregulated in many cancers.
274 Further, RNA expression data from 33 different cancer types, compiled in the GEPIA
275 atlas [69, 70], shows significantly elevated JPT2 mRNA levels in the majority of tumor
276 types (**Figure 4A**). One of the highest expression levels in non-cancerous cells occurs
277 in blood cells, which is noteworthy given the two photolabeling studies that identified
278 JPT2 employed different types of blood cells [14, 15].

279

280 Experimental analyses consistently show elevated JPT2 expression is associated with
281 increased cancer cell invasiveness, metastasis, and poorer survival [63, 68]. For
282 example, in non-small cell lung cancer, overexpression of JPT2 was detected in the
283 majority of patient tumor samples compared with non-tumor controls, and elevated
284 expression of JPT2 positively correlated with tumor size and poor prognosis [66].
285 Reciprocally, knockdown of JPT2 in several models inhibited cell proliferation,
286 migration, and tumor growth – again an effect seen in several different cancers [63, 64,
287 68]. For example, knockdown of JPT2 was associated with decreased tumorigenesis
288 and metastasis of hepatocellular carcinoma cells *in vivo* [53]. Altogether, higher JPT2
289 expression often correlates with poorer clinical prognosis. **Figure 4B** provides an
290 example of a disease-free survival plot for low-grade glioma for different JPT2
291 expression backgrounds.

292

293 Over 75 JPT2 mutants are detailed in the Cancer Genome Atlas, with approximately
294 one quarter of breast cancer patients harboring JPT2 mutations [64]. How different

295 JPT2 mutants [65] and JPT2 isoforms impact NAADP binding, TPC association, and
296 cellular growth phenotypes merits exploration. While all this evidence implies similar
297 associations of JPT2 and TPCs in tumorigenesis, some caution is needed. TPCs can
298 function independently from any involvement of NAADP: they are activated by PI(3,5)P₂
299 to evoke endolysosomal Na⁺ currents [7]. Equally, while JPT2 is implicated in multiple
300 pathways of cell growth and division, it is not yet known whether NAADP binding is
301 needed for JPT2 functionality in these pathways [63, 64, 66].

302

303 *Defining the JPT2 interactome*

304 Finally, identification of JPT2 lifts the veil on a broader JPT2 interactome. Multiple JPT2
305 interactors are predicted from various screening analyses [71, 72], although each of
306 these candidates requires further validation. The role of these JPT2 interacting proteins
307 could be critical for controlling TPC activity, for example by regulating the NAADP-
308 binding affinity of JPT2 or by controlling the subcellular localization of JPT2. In addition,
309 interactors could sequester JPT2 away from TPCs until appropriate physiological stimuli
310 are sensed. Again, this will be a key area to explore.

311

312 **A growing family of NAADP-BPs**

313 Further excitement surrounds the identification of a second NAADP-BP, LSM12, which
314 is a member of the 'like-Sm' RNA-binding protein family [16, 73]. LSM12 was resolved
315 as the only shared candidate between the TPC and NAADP interactomes, and was
316 shown to bind NAADP with high affinity (K_d for NAADP ~30nM) and selectivity over
317 NADP [16]. Additional support for LSM12 as an NAADP-BP includes (i) NAADP
318 conjugated to agarose beads was unable to interact with either TPC1 or TPC2 in the
319 absence of LSM12, (ii) NAADP-evoked Na⁺ currents and NAADP-evoked Ca²⁺ signals
320 were absent in LSM12 knockout HEK cell line overexpressing TPC2, but responses
321 could be restored by reconstituting LSM12 expression or injection of recombinant
322 protein, and (iii) LSM12 functionality required its LSM domain and endogenous NAADP-
323 evoked Ca²⁺ release was compromised in MEFs derived from transgenic mice where a
324 short sequence in the LSM domain was deleted [16]. Expression of LSM12 mRNA, like
325 JPT2, shows low tissue specificity (**Figure 3**) [45]. LSM12 mRNA is also upregulated in

326 many different tumors (**Figure 4C**), often in the same cancer types that exhibit
327 increased JPT2 expression [69, 70]. As a result, LSM12 upregulation is also correlated
328 with poor clinical outcomes (**Figure 4D**).

329
330 With these two NAADP-BPs now identified, it merits comment that neither JPT2 nor
331 LSM12 featured in previously published TPC proteomic datasets [30, 31, 74].
332 Conditions under which these prior proteomic studies were performed may not have
333 been optimal to capture the dynamics of NAADP-BP association with TPCs.
334 Alternatively, other necessary components of the interacting complex may yet to be
335 revealed. Equally unresolved is the nature of relationship between JPT2 and LSM12.
336 Do they physically interact? Knockdown of either NAADP-BP individually, even though
337 the other remains, appears sufficient to block endogenous NAADP-evoked Ca^{2+} signals,
338 and both independently bind NAADP [14, 16], but the presence of both seems to be
339 necessary to support NAADP action. Does this imply they partner in a complex, or do
340 they function epistatically in pathways of TPC activation or inactivation? If they do not
341 physically interact, how do they interact functionally? How does the presence of both
342 NAADP-BPs shape cellular responsiveness to NAADP?

343
344 The discovery of JPT2 and LSM12 further begs the question of whether there are more
345 NAADP-BPs to be unmasked? Beyond enzymes that metabolize NAADP, the existence
346 of additional NAADP-BPs that function as signal transducers seems likely. In support of
347 an expanded family of NAADP-BPs, photolabeling analyses in sea urchin egg
348 homogenates [17, 75], has resolved invertebrate NAADP-BPs with molecular weights
349 (45kDa, 40kDa, and 30kDa) distinct from the ~23kDa NAADP-BPs identified in
350 mammalian cells [24]. These sea urchin NAADP-BPs also binds NAADP with high
351 affinity and selectivity, exhibit the known pharmacology of NAADP-evoked Ca^{2+} release
352 and NAADP binding properties (irreversibility in high K^+), and immunoprecipitate with
353 sea urchin TPCs [24]. The identity of these urchin NAADP-BPs, and consequently any
354 relationship to JPT2 and LSM12, is currently unknown.

355

356 Therefore, it seems plausible that more NAADP-BPs will be discovered, such that the
357 appropriate question may not be how many, but what are their functional niches? While
358 the currently accepted paradigm of NAADP action culminates in TPC activation, TPCs
359 may be just one type of effector engaged by NAADP-liganded NAADP-BPs. This is
360 shown by the work of Roggenkamp *et al.* which implicates an interaction between JPT2
361 and RyR1 [15, 32]. However, the roles of the NAADP-BPs may extend beyond
362 regulation of Ca²⁺ dynamics such that other functional outputs, yet to be appreciated,
363 will emerge. For example, in *Drosophila*, which lacks TPCs, JPT already has its own
364 identity as a microtubule-binding protein [76]. Does *Drosophila* JPT bind NAADP? If so,
365 to what effect? Additionally, Gunaratne *et al.* [14] isolated JPT2 from erythrocytes, a cell
366 type where organelles and intracellular Ca²⁺ channels are absent, but NAADP is
367 present [77]. What is the function of JPT2 in red blood cells? By analogy with another
368 family of second messenger binding proteins - inositol polyphosphate binding proteins
369 [78], or to the STIM family of Ca²⁺ sensors that bind multiple different Ca²⁺ channels [79]
370 – a broader family of NAADP-BPs may fulfill pleiotropic messenger roles beyond
371 engagement of TPCs. This will be an important area of study now that the identity of
372 these NAADP-BPs is established.

373

374 **New tools**

375 Identification of both NAADP-BPs provides new opportunities to monitor and manipulate
376 NAADP signaling. For example, the NAADP binding modules in each NAADP-BP can
377 potentially be engineered into NAADP sensors able to report NAADP dynamics in intact
378 cells. This approach has been successfully realized for other second messengers,
379 including IP₃ and cAMP through the development of FRET-based reporters [80, 81].
380 Such tools could resolve the spatiotemporal dynamics of NAADP in intact cells and to
381 monitor the spatiotemporal relationship between NAADP and Ca²⁺ dynamics.
382 Fluorescence-based NAADP reporters would also be enabling of higher throughput
383 screening applications with the goal of identifying agonists coupled to NAADP
384 generation. Therefore, the development of reporters for NAADP will be a powerful new
385 approach to enable a transition away from the traditional radioligand-based approaches.
386 The identification of the NAADP-BPs also affords opportunity to develop new ligands to

387 manipulate this signaling pathway. This includes ligands that interact with the NAADP
388 binding site(s) on each NAADP-BP, as well as ligands that act at the binding interfaces
389 between NAADP-BPs and TPCs. The identification of the NAADP-BPs provides a
390 molecular framework to explore these druggable interfaces through modelling and
391 screening activities.

392
393 NAADP is a **biased agonist**, and evokes a significant Ca^{2+} permeability through TPCs,
394 while $\text{PI}(3,5)\text{P}_2$ activation results in a monovalent Na^+ flux [10]. These dual agonists
395 therefore trigger unique responses from the same ion channel target [82, 83], analogous
396 to the phenomenon of biased signaling that is well elaborated at G-protein-coupled
397 receptors (GPCRs) [84]. Are the NAADP-BPs the critical effectors of this signaling bias
398 by transducing the effects of their engaged ligands to stabilize a specific conformation of
399 TPC subunits and pore architecture that supports the characteristic Ca^{2+} permeability
400 diagnostic of NAADP action. Of interest is recent work identifying novel TPC2
401 chemotypes (e.g. TPC2-A1-N, **Box 1**) that mimic NAADP action [10, 85], though it
402 remains to be determined how TPC2-A1-N functions as a NAADP mimetic. It may act
403 like NAADP and bind NAADP-BPs that interact with TPC2, or it may act as an NAADP-
404 BP mimetic engaging TPC2 at the NAADP-BP interaction site. Alternatively, it could
405 work through another undescribed mechanism. Irrespective of these answers, these
406 ligands provide a clear example of progress in developing agents to manipulate the
407 function of the TPC complex, and the identification of NAADP-BPs spurs additional
408 possibilities for tool development. This effort may realize therapeutic benefit in diseases
409 where NAADP dysfunction is established [86].

410

411 **Concluding remarks**

412 The recent identification of two mammalian NAADP-BPs, after a decade long search, is
413 an exciting development for the NAADP signaling field. These discoveries provide new
414 impetus to understand and manipulate NAADP action in different cells and tissues, and
415 to resolve how NAADP signaling is perturbed in disease states. With these NAADP-BPs
416 finally yielding their identity, many new questions are accessible about structural
417 mechanism, regulatory control, functional impact, and cell biology of both NAADP-BPs

418 (see [Outstanding Questions](#)). These questions have become open to interrogation
419 now the identity of the NAADP-BP candidates is known. It will be an exciting journey to
420 explore wherever these discoveries lead.

421 **Acknowledgements:** Work supported by NIH-GM088790 and NSF-2027748 (to JSM).
422 R15-GM131329 (to JTS). SP was supported by BBSRC grants (BB/N01524X/1;
423 BB/T015853/1).

424 **References**

- 425 1. Lee, H.C. (2005) Nicotinic acid adenine dinucleotide phosphate (NAADP)-mediated
426 calcium signaling. *J Biol Chem* 280 (40), 33693-6.
- 427 2. Patel, S. (2015) Function and dysfunction of two-pore channels. *Sci Signal* 8 (384),
428 re7.
- 429 3. Calcraft, P.J. et al. (2009) NAADP mobilizes calcium from acidic organelles through
430 two-pore channels. *Nature* 459 (7246), 596-600.
- 431 4. Brailoiu, E. et al. (2009) Essential requirement for two-pore channel 1 in NAADP-
432 mediated calcium signaling. *J Cell Biol* 186 (2), 201-9.
- 433 5. Marchant, J.S. and Patel, S. (2015) Two-pore channels at the intersection of
434 endolysosomal membrane traffic. *Biochem Soc Trans* 43 (3), 434-41.
- 435 6. Freeman, S.A. et al. (2020) Lipid-gated monovalent ion fluxes regulate endocytic
436 traffic and support immune surveillance. *Science* 367 (6475), 301-305.
- 437 7. Wang, X. et al. (2012) TPC proteins are phosphoinositide- activated sodium-selective
438 ion channels in endosomes and lysosomes. *Cell* 151 (2), 372-83.
- 439 8. Cang, C. et al. (2013) mTOR regulates lysosomal ATP-sensitive two-pore Na(+)
440 channels to adapt to metabolic state. *Cell* 152 (4), 778-790.
- 441 9. Ruas, M. et al. (2015) Expression of Ca(2+)-permeable two-pore channels rescues
442 NAADP signalling in TPC-deficient cells. *EMBO J* 34 (13), 1743-58.
- 443 10. Gerndt, S. et al. (2020) Agonist-mediated switching of ion selectivity in TPC2
444 differentially promotes lysosomal function. *Elife* 9, 10.7554/eLife.54712.
- 445 11. She, J. et al. (2018) Structural insights into the voltage and phospholipid activation
446 of the mammalian TPC1 channel. *Nature* 556 (7699), 130-134.
- 447 12. She, J. et al. (2019) Structural mechanisms of phospholipid activation of the human
448 TPC2 channel. *Elife* 8, 10.7554/eLife.45222.
- 449 13. Patel, S. (2018) Two-pore channels open up. *Nature* 556 (7699), 38-40.
- 450 14. Gunaratne, G.S. et al. (2021) Essential requirement for JPT2 in NAADP-evoked
451 Ca(2+) signaling. *Sci Signal* 14 (675).
- 452 15. Roggenkamp, H.G. et al. (2021) HN1L/JPT2: A signaling protein that connects
453 NAADP generation to Ca(2+) microdomain formation. *Sci Signal* 14 (675).
- 454 16. Zhang, J. et al. (2021) Lsm12 is an NAADP receptor and a two-pore channel
455 regulatory protein required for calcium mobilization from acidic organelles. *Nat Commun*
456 12 (1), 4739.

- 457 17. Galione, A. et al. (2014) Preparation and use of sea urchin egg homogenates for
458 studying NAADP-mediated Ca(2+)(+) release. Cold Spring Harb Protoc 2014 (9), 988-92.
- 459 18. Yuan, Y. et al. (2019) Probing Ca(2+) release mechanisms using sea urchin egg
460 homogenates. Methods Cell Biol 151, 445-458.
- 461 19. Aarhus, R. et al. (1996) Activation and inactivation of Ca2+ release by NAADP+. J
462 Biol Chem 271 (15), 8513-6.
- 463 20. Berridge, G. et al. (2002) Solubilization of receptors for the novel Ca2+-mobilizing
464 messenger, nicotinic acid adenine dinucleotide phosphate. J Biol Chem 277 (46),
465 43717-23.
- 466 21. Patel, S. et al. (2000) Widespread distribution of binding sites for the novel Ca2+-
467 mobilizing messenger, nicotinic acid adenine dinucleotide phosphate, in the brain. J Biol
468 Chem 275 (47), 36495-7.
- 469 22. Bak, J. et al. (2001) NAADP receptors are present and functional in the heart. Curr
470 Biol 11 (12), 987-90.
- 471 23. Zong, X. et al. (2009) The two-pore channel TPCN2 mediates NAADP-dependent
472 Ca(2+)-release from lysosomal stores. Pflugers Arch 458 (5), 891-9.
- 473 24. Walseth, T.F. et al. (2012) Photoaffinity labeling of high affinity nicotinic acid
474 adenine dinucleotide phosphate (NAADP)-binding proteins in sea urchin egg. J Biol
475 Chem 287 (4), 2308-15.
- 476 25. Lin-Moshier, Y. et al. (2012) Photoaffinity labeling of nicotinic acid adenine
477 dinucleotide phosphate (NAADP) targets in mammalian cells. J Biol Chem 287 (4),
478 2296-307.
- 479 26. Marchant, J.S. et al. (2012) The Molecular Basis for Ca(2+) Signalling by NAADP:
480 Two-Pore Channels in a Complex? Messenger (Los Angel) 1 (1), 63-76.
- 481 27. Walseth, T.F. et al. (2012) Nicotinic Acid Adenine Dinucleotide 2'-Phosphate
482 (NAADP) Binding Proteins in T-Lymphocytes. Messenger (Los Angel) 1 (1), 86-94.
- 483 28. Gunaratne, G.S. et al. (2019) 5-Azido-8-ethynyl-NAADP: A bifunctional, clickable
484 photoaffinity probe for the identification of NAADP receptors. Biochim Biophys Acta Mol
485 Cell Res 1866 (7), 1180-1188.
- 486 29. Asfaha, T.Y. et al. (2019) The synthesis and characterization of a clickable-
487 photoactive NAADP analog active in human cells. Cell Calcium 83, 102060.
- 488 30. Lin-Moshier, Y. et al. (2014) The Two-pore channel (TPC) interactome unmasks
489 isoform-specific roles for TPCs in endolysosomal morphology and cell pigmentation.
490 Proc Natl Acad Sci U S A 111 (36), 13087-92.

- 491 31. Krogsaeter, E.K. et al. (2019) The protein interaction networks of mucolipins and
492 two-pore channels. *Biochim Biophys Acta Mol Cell Res* 1866 (7), 1111-1123.
- 493 32. Walseth, T.F. and Guse, A.H. (2021) NAADP: From Discovery to Mechanism. *Front*
494 *Immunol* 12, 703326.
- 495 33. Zhou, G. et al. (2004) Cloning, expression and subcellular localization of HN1 and
496 HN1L genes, as well as characterization of their orthologs, defining an evolutionarily
497 conserved gene family. *Gene* 331, 115-23.
- 498 34. Chi, Y. et al. (2008) Identification of CDK2 substrates in human cell lysates.
499 *Genome Biol* 9 (10), R149.
- 500 35. Brailoiu, E. et al. (2010) An NAADP-gated two-pore channel targeted to the plasma
501 membrane uncouples triggering from amplifying Ca²⁺ signals. *J Biol Chem* 285 (49),
502 38511-6.
- 503 36. Pitt, S.J. et al. (2010) TPC2 Is a Novel NAADP-sensitive Ca²⁺ Release Channel,
504 Operating as a Dual Sensor of Luminal pH and Ca²⁺. *J Biol Chem* 285 (45), 35039-
505 35046.
- 506 37. Rybalchenko, V. et al. (2012) Membrane potential regulates nicotinic acid adenine
507 dinucleotide phosphate (NAADP) dependence of the pH- and Ca²⁺-sensitive organellar
508 two-pore channel TPC1. *J Biol Chem* 287 (24), 20407-16.
- 509 38. Berg, I. et al. (2000) Nicotinic acid adenine dinucleotide phosphate (NAADP(+)) is
510 an essential regulator of T-lymphocyte Ca(2+)-signaling. *J Cell Biol* 150 (3), 581-8.
- 511 39. Guse, A.H. (2012) Linking NAADP to ion channel activity: a unifying hypothesis. *Sci*
512 *Signal* 5 (221), pe18.
- 513 40. Galione, A. (2015) A primer of NAADP-mediated Ca(2+) signalling: From sea urchin
514 eggs to mammalian cells. *Cell Calcium* 58 (1), 27-47.
- 515 41. Marchant, J.S. and Patel, S. (2013) Questioning regulation of two-pore channels by
516 NAADP. *Messenger (Los Angel)* 2 (2), 113-119.
- 517 42. Morgan, A.J. et al. (2015) TPC: the NAADP discovery channel? *Biochem Soc Trans*
518 43 (3), 384-9.
- 519 43. Kumada, T. et al. (2010) Ttyh1, a Ca(2+)-binding protein localized to the
520 endoplasmic reticulum, is required for early embryonic development. *Dev Dyn* 239 (8),
521 2233-45.
- 522 44. Tang, W. et al. (1997) Murine Hn1 on chromosome 11 is expressed in hemopoietic
523 and brain tissues. *Mamm Genome* 8 (9), 695-6.

524 45. Consortium, G.T. (2015) Human genomics. The Genotype-Tissue Expression
525 (GTEx) pilot analysis: multitissue gene regulation in humans. *Science* 348 (6235), 648-
526 60.

527 46. Kelu, J.J. et al. (2018) TPC2-mediated Ca(2+) signaling is required for the
528 establishment of synchronized activity in developing zebrafish primary motor neurons.
529 *Dev Biol* 438 (1), 57-68.

530 47. Brailoiu, E. et al. (2006) Messenger-specific role for nicotinic acid adenine
531 dinucleotide phosphate in neuronal differentiation. *J Biol Chem* 281 (23), 15923-8.

532 48. Zhang, Z.H. et al. (2013) Two pore channel 2 differentially modulates neural
533 differentiation of mouse embryonic stem cells. *PLoS One* 8 (6), e66077.

534 49. Edfors, F. et al. (2016) Gene-specific correlation of RNA and protein levels in human
535 cells and tissues. *Mol Syst Biol* 12 (10), 883.

536 50. Zhang, J. et al. (2020) Lsm12 is an NAADP receptor and a two-pore channel
537 regulatory protein required for calcium mobilization from acidic organelles. *bioRxiv*,
538 <https://doi.org/10.1101/2020.05.21.109850>

539 51. Chen, W. et al. (2020) The functions and targets of miR-212 as a potential
540 biomarker of cancer diagnosis and therapy. *J Cell Mol Med* 24 (4), 2392-2401.

541 52. Sun, S. et al. (2018) MicroRNA-212-5p Prevents Dopaminergic Neuron Death by
542 Inhibiting SIRT2 in MPTP-Induced Mouse Model of Parkinson's Disease. *Front Mol*
543 *Neurosci* 11, 381.

544 53. Li, L. et al. (2019) HN1L-mediated transcriptional axis AP-2gamma/METTL13/TCF3-
545 ZEB1 drives tumor growth and metastasis in hepatocellular carcinoma. *Cell Death Differ*
546 26 (11), 2268-2283.

547 54. Grimm, C. et al. (2018) Endolysosomal Cation Channels and Cancer-A Link with
548 Great Potential. *Pharmaceuticals (Basel)* 11 (1), 10.3390/ph11010004.

549 55. Faris, P. et al. (2018) Endolysosomal Ca(2+) Signalling and Cancer Hallmarks: Two-
550 Pore Channels on the Move, TRPML1 Lags Behind! *Cancers (Basel)* 11 (1), 27.

551 56. Alharbi, A.F. and Parrington, J. (2019) Endolysosomal Ca(2+) Signaling in Cancer:
552 The Role of TPC2, From Tumorigenesis to Metastasis. *Front Cell Dev Biol* 7, 302.

553 57. Sakurai, Y. et al. (2015) Ebola virus. Two-pore channels control Ebola virus host cell
554 entry and are drug targets for disease treatment. *Science* 347 (6225), 995-8.

555 58. Gunaratne, G.S. et al. (2018) NAADP-dependent Ca(2+) signaling regulates Middle
556 East respiratory syndrome-coronavirus pseudovirus translocation through the
557 endolysosomal system. *Cell Calcium* 75, 30-41.

558 59. Ou, X. et al. (2020) Characterization of spike glycoprotein of SARS-CoV-2 on virus
559 entry and its immune cross-reactivity with SARS-CoV. *Nat Commun* 11 (1), 1620.

560 60. Gunaratne, G.S. et al. (2018) A screening campaign in sea urchin egg homogenate
561 as a platform for discovering modulators of NAADP-dependent Ca(2+) signaling in
562 human cells. *Cell Calcium* 75, 42-52.

563 61. Johnston, G.P. et al. (2019) Nipah Virus-Like Particle Egress Is Modulated by
564 Cytoskeletal and Vesicular Trafficking Pathways: a Validated Particle Proteomics
565 Analysis. *mSystems* 4 (5), 10.1128/mSystems.00194-19.

566 62. Lei, J. et al. (2019) HN1L is essential for cell growth and survival during
567 nucleopolyhedrovirus infection in silkworm, *Bombyx mori*. *PLoS One* 14 (5), e0216719.

568 63. Jiao, D. et al. (2021) HN1L promotes migration and invasion of breast cancer by up-
569 regulating the expression of HMGB1. *J Cell Mol Med* 25 (1), 397-410.

570 64. Liu, Y. et al. (2018) HN1L Promotes Triple-Negative Breast Cancer Stem Cells
571 through LEPR-STAT3 Pathway. *Stem Cell Reports* 10 (1), 212-227.

572 65. Liu, Z.B. et al. (2019) Detection of breast cancer stem cell gene mutations in
573 circulating free DNA during the evolution of metastases. *Breast Cancer Res Treat* 178
574 (2), 251-261.

575 66. Li, L. et al. (2017) Overexpression of HN1L promotes cell malignant proliferation in
576 non-small cell lung cancer. *Cancer Biol Ther* 18 (11), 904-915.

577 67. Petroziello, J. et al. (2004) Suppression subtractive hybridization and expression
578 profiling identifies a unique set of genes overexpressed in non-small-cell lung cancer.
579 *Oncogene* 23 (46), 7734-45.

580 68. Wang, Z.Y. et al. (2021) HN1L promotes invasion and metastasis of the
581 esophagogastric junction adenocarcinoma. *Thorac Cancer* 12 (5), 650-658.

582 69. Tang, Z. et al. (2017) GEPIA: a web server for cancer and normal gene expression
583 profiling and interactive analyses. *Nucleic Acids Res* 45 (W1), W98-W102.

584 70. Tang, Z. et al. (2019) GEPIA2: an enhanced web server for large-scale expression
585 profiling and interactive analysis. *Nucleic Acids Res* 47 (W1), W556-W560.

586 71. Oughtred, R. et al. (2021) The BioGRID database: A comprehensive biomedical
587 resource of curated protein, genetic, and chemical interactions. *Protein Sci* 30 (1), 187-
588 200.

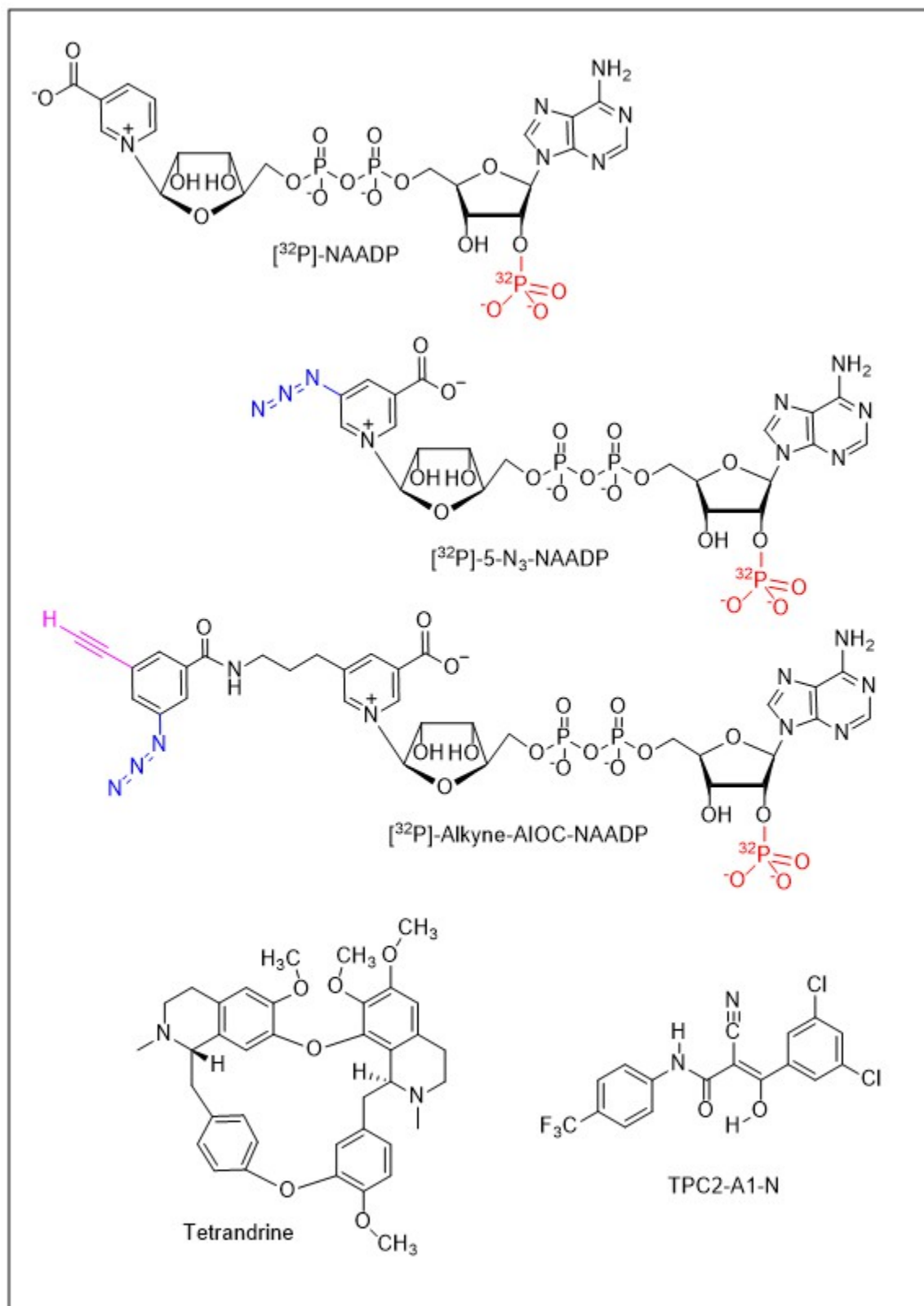
589 72. Murali, T. et al. (2011) Droid 2011: a comprehensive, integrated resource for
590 protein, transcription factor, RNA and gene interactions for *Drosophila*. *Nucleic Acids*
591 *Res* 39 (Database issue), D736-43.

- 592 73. Lekontseva, N.V. et al. (2021) Diversity of LSM Family Proteins: Similarities and
593 Differences. *Biochemistry-Moscow* 86 (Suppl 1), S38-S49.
- 594 74. Grimm, C. et al. (2014) High susceptibility to fatty liver disease in two-pore channel
595 2-deficient mice. *Nat Commun* 5, 4699.
- 596 75. May, J.M. (2012) Vitamin C transport and its role in the central nervous system.
597 *Subcell Biochem* 56, 85-103.
- 598 76. Karpova, N. et al. (2006) Jupiter, a new *Drosophila* protein associated with
599 microtubules. *Cell Motil Cytoskeleton* 63 (5), 301-12.
- 600 77. Churamani, D. et al. (2004) Determination of cellular nicotinic acid-adenine
601 dinucleotide phosphate (NAADP) levels. *Biochem J* 380 (Pt 2), 449-54.
- 602 78. Wu, M. et al. (2016) Inositol polyphosphates intersect with signaling and metabolic
603 networks via two distinct mechanisms. *Proc Natl Acad Sci U S A* 113 (44), E6757-
604 E6765.
- 605 79. Cahalan, M.D. (2010) Cell biology. How to STIMulate calcium channels. *Science*
606 330 (6000), 43-4.
- 607 80. Miyamoto, A. and Mikoshiba, K. (2017) Probes for manipulating and monitoring IP3.
608 *Cell Calcium* 64, 57-64.
- 609 81. Kim, N. et al. (2021) cAMP Biosensors Based on Genetically Encoded
610 Fluorescent/Luminescent Proteins. *Biosensors (Basel)* 11 (2).
- 611 82. Chung, M.K. et al. (2008) TRPV1 shows dynamic ionic selectivity during agonist
612 stimulation. *Nat Neurosci* 11 (5), 555-64.
- 613 83. Herrington, J. and Arey, B.J. (2014) Conformational Mechanisms of Signaling Bias
614 of Ion Channels. In *Biased Signaling in Physiology, Pharmacology and Therapeutics*
615 (Arey, B.J. ed), pp. 173-207, Academic Press.
- 616 84. Wootten, D. et al. (2018) Mechanisms of signalling and biased agonism in G
617 protein-coupled receptors. *Nat Rev Mol Cell Biol* 19 (10), 638-653.
- 618 85. Gerndt, S. et al. (2020) Discovery of lipophilic two-pore channel agonists. *FEBS J*
619 287 (24), 5284-5293.
- 620 86. Patel, S. and Kilpatrick, B.S. (2018) Two-pore channels and disease. *Biochim*
621 *Biophys Acta Mol Cell Res* 1865 (11 Pt B), 1678-1686.
- 622 87. Muller, M. et al. (2021) Gene editing and synthetically accessible inhibitors reveal
623 role for TPC2 in HCC cell proliferation and tumor growth. *Cell Chem Biol* 28 (8), 1119-
624 1131 e27.

- 625 88. Clementi, N. et al. (2021) Naringenin is a powerful inhibitor of SARS-CoV-2 infection
626 in vitro. *Pharmacol Res* 163, 105255.
- 627 89. Khan, N. et al. (2020) Two-pore channels regulate Tat endolysosome escape and
628 Tat-mediated HIV-1 LTR transactivation. *FASEB J* 34 (3), 4147-4162.
- 629 90. Ruas, M. et al. (2010) Purified TPC isoforms form NAADP receptors with distinct
630 roles for Ca(2+) signaling and endolysosomal trafficking. *Curr Biol* 20 (8), 703-9.
- 631 91. Penny, C.J. et al. (2019) Mining of Ebola virus entry inhibitors identifies approved
632 drugs as two-pore channel pore blockers. *Biochim Biophys Acta Mol Cell Res* 1866 (7),
633 1151-1161.
- 634 92. Daniloski, Z. et al. (2021) Identification of Required Host Factors for SARS-CoV-2
635 Infection in Human Cells. *Cell* 184 (1), 92-105 e16.
- 636 93. Pafumi, I. et al. (2017) Naringenin Impairs Two-Pore Channel 2 Activity And Inhibits
637 VEGF-Induced Angiogenesis. *Sci Rep* 7 (1), 5121.
- 638 94. Favia, A. et al. (2014) VEGF-induced neoangiogenesis is mediated by NAADP and
639 two-pore channel-2-dependent Ca²⁺ signaling. *Proc Natl Acad Sci U S A* 111 (44),
640 E4706-15.
- 641 95. Nguyen, O.N. et al. (2017) Two-Pore Channel Function Is Crucial for the Migration
642 of Invasive Cancer Cells. *Cancer Res* 77 (6), 1427-1438.
- 643 96. D'Amore, A. et al. (2020) Loss of Two-Pore Channel 2 (TPC2) Expression Increases
644 the Metastatic Traits of Melanoma Cells by a Mechanism Involving the Hippo Signalling
645 Pathway and Store-Operated Calcium Entry. *Cancers (Basel)* 12 (9).
- 646
- 647
- 648

649
650

BOX 1: A chemical toolbox for probing NAADP action.



651

652 [³²P]-Nicotinic acid adenine dinucleotide phosphate (NAADP; top left) represents one
653 version of a radioisotope (red) used to study NAADP binding in cells and tissues. [³²P]-
654 5-N₃-NAADP was the original photoaffinity probe used to characterize NAADP targets
655 [24, 25]. The probe incorporates a photoreactive azide group (blue) to crosslink binding
656 partners following ultraviolet irradiation. [³²P]-alkyne-‘all-in-one-click’ (AIOC)-NAADP is a
657 bifunctional probe that incorporates an additional clickable alkynyl moiety (magenta) to
658 couple photolabeling to NAADP-BP enrichment. For example, to isolate JPT2 [14],
659 photoprobe-bound NAADP-BPs were biotinylated via a copper-catalyzed alkyne-azide
660 cycloaddition (CuAAC) using ‘click chemistry’ such that the biotinylated proteins could
661 then be captured using neutravidin. Tetrandrine is a bisbenzylisoquinoline alkaloid
662 originally shown to block TPCs [57], with other derivatives of this chemotype also
663 blocking two-pore channel (TPC) function [58, 87]. TPC2-A1-N is a novel chemotype
664 recently identified in a drug screen profiling TPC2 that mimics NAADP-evoked Ca²⁺
665 signals and NAADP-evoked TPC currents [10].

BOX 2: Two-pore channels (TPCs) in viral infection and cancer.

There is growing evidence that TPCs control viral trafficking through the endolysosomal system [14, 57-59, 88, 89]. This role of TPCs was first shown by Sakurai *et al.* who validated TPCs as druggable targets that blocked Ebola virus infection [57]. Their work identified the natural product tetrandrine (a bisbenzylisoquinoline alkaloid) as a TPC antagonist which inhibited Ebolavirus infectivity *in vitro* and in a mouse model [57]. Genetic knockdown, or knockout of TPC1 or TPC2 also prevented Ebolavirus entry *in vitro* [57]. Mechanistically these effects relate to the role of TPCs in regulating vesicular fusion events between different compartments of the endolysosomal system, through which diverse pathogens traverse to gain cytoplasmic access [5, 57, 74, 90]. Subsequent work using a related bisbenzylisoquinoline (fangchinoline) demonstrated that TPC inhibition blocked infectivity of a pseudotyped Middle East Respiratory Syndrome coronavirus (MERS-CoV) [58, 60]. The potency of various blockers at inhibiting NAADP-evoked Ca^{2+} release correlated well with the extent of inhibition of viral infectivity [60]. Knockdown or chemical blockade of TPCs also blocked infection of a SARS-CoV-2 pseudovirus, an outcome also seen in assays using wild-type, replication-competent SARS-CoV-2 [59, 88]. *In silico* analyses suggest that several known anti-viral agents may act as TPC ligands [91]. Genome-wide CRISPR screening found that knockout of TPC1 inhibited infectivity of authentic SARS-CoV-2 in human alveolar epithelial cells [92].

Emerging data implicates TPCs in multiple aspects of tumorigenesis [87, 93-95]. In early stages of tumorigenesis, TPCs promote tumor growth, the secretion of enzymes that degrade extracellular components, cell migration and invasiveness. TPCs act as nutrient sensors, regulating autophagy and energy metabolism: TPC2 biases pathways of cellular energy usage to promote proliferation [87] while also enhancing tumor growth by stimulating new blood vessel formation [93, 94]. Knockdown, or pharmacological blockade, of either TPC1 or TPC2 reduces cell attachment and migration in several human cell lines by disrupting β 1-integrin trafficking to the leading edge of migrating cells [95]. Knockout of TPC2 is sufficient to impair proliferation and migration of RIL175 cells (a mouse hepatocellular carcinoma cell line) *in vitro* and block tumor growth *in vivo* [87]. Anti-tumor effects are also seen after pharmacological inhibition of TPC2: treatment of mice with a new TPC2 blocker (SG-094, a smaller derivative of the same bisbenzylisoquinoline chemotype) inhibited tumor growth [87]. Importantly, the role of TPCs may depend on the stage of tumor advancement. In late-stage metastatic melanoma, TPC2 knockout increased invasiveness and enzyme secretion [96]. Understanding the role of TPCs throughout the tumorigenic process and in multiple tumor types will be the focus of much future work.

Collectively, these studies highlight the promise of TPCs as druggable targets for both antivirals and chemotherapeutics. Antiviral and anticancer effects are seen with several of the same compounds that target TPC function.

711 **Figure Legends**

712

713 **Figure 1. The action of nicotinic acid adenine dinucleotide phosphate (NAADP)-**
714 **binding proteins (BPs) and emerging questions enabled by their identification. (A)**

715 Two-pore channels (TPCs) are ion channels expressed on endolysosomes. They are
716 subject to polymodal activation by NAADP, PI(3,5)P₂, and/or voltage (V). **(B)** Models for
717 TPC activation by NAADP. Top, the originally envisioned model that TPCs are directly
718 activated by the binding of NAADP has not received experimental support. Rather,
719 NAADP has been proposed to activate TPCs indirectly by engaging NAADP-BPs
720 (purple) that are essential components for NAADP-triggered Ca²⁺ release. Bottom, this
721 may occur in several ways, for example by (i) NAADP association with the NAADP-BP
722 causing a translocation of NAADP-liganded NAADP-BPs to the TPC complex, or (ii) by
723 NAADP engaging NAADP-BPs already associated with the TPC complex. (iii)
724 Dissociation of the NAADP-BP from the channel complex, or dissociation of NAADP
725 from the NAADP-BP, could serve to terminate NAADP action. **(C)** Future areas for
726 NAADP-BP research enabled by the recent identification of two NAADP-BPs, JPT2 and
727 LSM12. These include: (1) the mechanism of JPT2 interaction of NAADP and JPT2
728 association with different TPC isoforms, (2) regulation of JPT2 expression levels, for
729 example through degradation, to set cellular NAADP sensitivity, (3) characterization of
730 other functions of JPT2 and the broader JPT2 interactome as a roadmap for
731 understanding new facets of NAADP biology, (4) identification and characterization of
732 additional vertebrate and invertebrate NAADP-BPs, (5) development of novel tools to
733 manipulate this signaling pathway. Each of these areas is discussed in the main text.
734 This figure was created with BioRender.com.

735

736 **Figure 2. JPT2 structure and evolution. (A)** Schematic representation of human JPT2

737 splice isoforms. Length in amino acids is shown. **(B)** **Cladogram of JPT sequences from**
738 **animals with bootstrap values shown.** Phylogenetics was performed as described in
739 <https://pubmed.ncbi.nlm.nih.gov/34608145/> using PHYML (version 3.1) with the JTT
740 amino acid substitution model, estimated proportion of invariable sites and the four-
741 category discrete gamma model (JTT + I + G) selected by ProtTest (Version 3.4.2).
742 Deuterostome branches are shaded in brown and protostome branches shades in
743 yellow. Abbreviations: CteJPT (ELU08900.1) *Capitella teleta*; HroJPT
744 (XP_009029441.1) *Helobdella robusta*; AcaJPT (XP_005102887.1) *Aplysia californica*;
745 PmaJPT (XP_033742783.1) *Pecten maximus*; OvuJPT (XP_029648722.1) *Octopus*
746 *vulgaris*; TnaJPT (OUC50045.1) *Trichinella nativa*; DmeJPT (Q9I7K0) *Drosophila*
747 *melanogaster*; NpiJPT (AII97726.1) *Nephila pilipes*; CscJPT (XP_023222178.1)
748 *Centruroides sculpturatus*; DmaJPT (XP_032791280.1) *Daphnia magna*; AruJPT
749 (XP_033631490.1) *Asterias rubens*; AcanJPT (XP_022098988.1) *Acanthaster planci*;
750 SpuJPT (XP_011684190.1) *Strongylocentrotus purpuratus*; AjaJPT (PIK56568.1)
751 *Apostichopus japonicus*; AjapJPT (XP_033109709.1) *Anneissia japonica*; BflJPT
752 (XP_002611678.1) *Branchiostoma floridae*; CinJPT (XP_009861954.1) *Ciona*
753 *intestinalis*; PmamJPT (CAB3257823.1) *Phallusia mammillata*; OdiJPT (CBY20678.1)
754 *Oikopleura dioica*; PmarJPT (XP_032826119.1) *Petromyzon marinus*; AraJPT1
755 (XP_032900329.1), AraJPT2 (XP_032896233.1) *Amblyraja radiata*; DreJPT1a
756 (NP_001082982.1), DreJPT1b (NP_991176.1), DreJPT2 (NP_955869.2) *Danio rerio*;

757 LchJPT1 (XP_005998303.1), LchJPT2 (XP_005997850.1) *Latimeria chalumnae*;
758 XtrJPT1 (NP_001139220.1), XtrJPT2 (XP_012825626.1) *Xenopus tropicalis*; AcarJPT1
759 (XP_003217263.1), AcarJPT2 (XP_008120328.1) *Anolis carolinensis*; GgaJPT1
760 (XP_015150886.1), GgaJPT2 (NP_001265082.1) *Gallus gallus*; CluJPT1
761 (NP_001093413.1), CluJPT2 (XP_022275981.1) *Canis lupus familiaris*; MmuJPT1
762 (NP_032284.1), MmuJPT2 (NP_945175.1) *Mus musculus*; HsaJPT1
763 (NP_001002032.1), HsaJPT2 (NP_653171.1) *Homo sapiens*.

764

765 **Figure 3. NAADP-BP expression.** (A) Violin plot showing expression values (TPM,
766 transcripts per million) for JPT2 (brown) and LSM12 (blue) across a variety of tissues,
767 calculated from a gene model where all isoforms are collapsed to a single gene. Box
768 plots show median as well as 25th and 75th percentiles. TPM values were produced
769 with RNA-SeQC v1.1.9. Noticeably, expression of both NAADP-BPs shows a broad
770 tissue distribution, with increased JPT2 expression is seen in spinal cord, as described
771 in the main text. (B) Heatmap depicting median TPMs for NAADP-BPs (JPT2, LSM12)
772 as well as two-pore channels TPCs (TPC1 and TPC2). Tissues are arrayed
773 alphabetically. These data show JPT2 expression is better correlated with TPC1, and
774 LSM12 with TPC2. Data for Figure 3 is reproduced from the Genotype-Tissue
775 Expression project (GTEx, v8, [45])

776

777 **Figure 4. JPT2 expression in cancer.** (A) Expression plot detailing JPT2 transcript
778 levels in 33 different tumors (red) compared with controls (green). Different cancers are
779 color-coded to indicate statistically higher JPT2 expression in cancerous (red) or normal
780 tissue (green) or no statistical difference (black). Mean expression (bar). Cancer
781 abbreviations: ACC (Adrenocortical carcinoma), BLCA (Bladder Urothelial Carcinoma),
782 BRCA (Breast invasive carcinoma), CESC (Cervical squamous cell carcinoma,
783 endocervical adenocarcinoma), CHOL (Cholangiocarcinoma), COAD (Colon
784 adenocarcinoma), DLBC (Lymphoid Neoplasm Diffuse Large B-cell Lymphoma), ESCA
785 (Esophageal carcinoma), GBM (Glioblastoma multiforme), HNSC (Head and Neck
786 squamous cell carcinoma), KICH (Kidney Chromophobe), KIRC (Kidney renal clear cell
787 carcinoma), KIRP (Kidney renal papillary cell carcinoma), LAML (Acute Myeloid
788 Leukemia), LGG (Brain Lower Grade Glioma), LIHC (Liver hepatocellular carcinoma),
789 LUAD (Lung adenocarcinoma), LUSC (Lung squamous cell carcinoma), MESO
790 (Mesothelioma), OV (Ovarian serous cystadenocarcinoma), PAAD (Pancreatic
791 adenocarcinoma), PCPG (Pheochromocytoma and Paraganglioma), PRAD (Prostate
792 adenocarcinoma), READ (Rectum adenocarcinoma), SARC (Sarcoma), SKCM (Skin
793 Cutaneous Melanoma), STAD (Stomach adenocarcinoma), TGCT (Testicular Germ Cell
794 Tumors), THCA (Thyroid carcinoma), THYM (Thymoma), UCEC (Uterine Corpus
795 Endometrial Carcinoma), UCS (Uterine Carcinosarcoma), UVM (Uveal Melanoma). (B)
796 Disease-free survival plot for high versus low JPT2 expression levels (median±50%
797 cutoffs) in LGG (n=257). Dotted lines (95% confidence). (C&D) Similar analyses for (C)
798 LSM12 expression and (D) outcomes in ACC (n=38). Expression and survival data for
799 Figure 4 are reproduced from GEPIA2 [69, 70].

800 **Glossary**

801

802

803 **NAADP:** Nicotinic acid adenine dinucleotide phosphate is a potent Ca^{2+} releasing
804 second messenger produced in response to cell stimulation. NAADP releases Ca^{2+} from
805 endosomes and lysosomes in many different organisms through activation of a family of
806 ion channels known as two pore channels (TPCs).

807

808 **NAADP-BP:** NAADP binding protein. In mammalian cells, unidentified ~23kDa proteins
809 resolved in photolabeling studies shown to possess properties and behavior that mimic
810 the characteristics of the NAADP Ca^{2+} release pathway. These NAADP-BPs are
811 postulated to confer NAADP sensitivity to TPCs by acting as TPC accessory proteins
812 necessary for NAADP-evoked Ca^{2+} release.

813

814 **JPT2:** Jupiter Microtubule Associated Homolog-2. One of two members of the Jupiter
815 gene family (*JPT1/HN1* and *JPT2/HN1L*) that has been shown to regulate cell
816 proliferation and survival. Recently identified as a NAADP-binding protein and TPC
817 accessory protein required for endogenous NAADP-evoked Ca^{2+} release and viral
818 trafficking.

819

820 **LSM12:** 'Like-Sm' protein 12. One member of the larger LSM protein family,
821 representatives of which are conserved evolutionarily from prokaryotes to humans. LSM
822 family members are traditionally viewed as having roles in post-transcriptional regulation
823 of RNA expression. Also recently identified as a NAADP-binding protein and TPC
824 accessory protein required for NAADP-evoked Ca^{2+} release.

825

826 **TPC:** Two pore channel. A class of voltage- and/or ligand-gated (activated by both
827 NAADP and $\text{PI}(3,5)\text{P}_2$) ion channels that is found intracellularly in endosomes and
828 lysosomes.

829

830 **Bifunctional photoprobe:** A chemical probe with dual functional groups used in
831 photolabeling studies. The first functionalized substituent is photoreactive to enable
832 light-evoked cross-linking with specific targets. The second functionalized substituent is
833 a moiety that enables an enrichment strategy to isolate the photolabeled target.

834

835 **Biased agonist.** A ligand that induces a receptor conformation that preferential couples
836 to a specific signaling outcome. Typically used for GPCRs in the context of G protein
837 versus β -arrestin coupling, but also applicable to ion channel signaling outcomes. Here,
838 NAADP act as a biased agonist as it evokes a Ca^{2+} flux through TPCs.